Representation and modeling of the Chilean electric power network for seismic resilience analysis

E. Ferrario[1,2], A. Poulos[2], J. C. de la Llera[1,2], A. Lorca[1], A. Oneto[1], C. Magnere[1]

[1]*Pontificia Universidad Católica de Chile*
[2]*National Research Center for Integrated Natural Disaster Management (CIGIDEN) CONICYT/FONDAP/15110017, Chile.*

Electric Power Networks (EPNs) are exposed to the occurrence of highly disruptive natural events such as large earthquakes. The physical damage to EPN components due to seismic events can seriously compromise the ability to generate, transmit, and distribute electricity to final users and to other interconnected critical infrastructures. In this context, resilience analysis is fundamental to identify the key components at risk to sustain or quickly restore the EPN functionality. This work presents a first step in the development of a detailed Chilean EPN model and illustrates an analysis framework to assess its resilience under the occurrence of earthquake scenarios. Specifically, the Chilean EPN model is built at a high level of detail using several Chilean data sources. Then, resilience of the network is assessed in four main steps: (1) generation of local intensity levels at the component sites; (2) evaluation of the earthquake impact on the EPN components using their fragilities; (3) evaluation of the component recovery time using downtime distributions; and (4) estimation of the EPN performance by means of simulating an optimal power flow model throughout the restoration process until service is fully restored. Results are expected to contribute toward a more resilient Chilean power network under seismic action.

Keywords: Electric Power Networks, Resilience, Earthquakes, Fragility Curves, Monte Carlo Simulation.

1. Introduction

Like most spatially distributed systems, Electric Power Networks (EPNs) are exposed to the occurrence of unexpected disruptive natural events such as large earthquakes (Southwell, 2014). Indeed, the evidence gathered from recent earthquakes confirms that physical damage to EPN components can seriously compromise the ability to generate, transmit, and distribute electricity to final users and to other interconnected Critical Infrastructures (CIs) such as water distribution systems, telecommunications, and healthcare systems (Araneda et al., 2010; Kröger and Zio, 2011; Dueñas-Osorio and Kwasinski, 2012; NRC, 2013). Interruptions in the electricity supply in the aftermath of a severe seismic event, directly translate into welfare and economic losses, and other social undesirable behaviors, deepening the already critical conditions of the affected population during the emergency (Araneda et al., 2010).

In particular, Chile is continuously exposed to various natural hazards and the estimated average annual loss due to earthquakes has been estimated at around 1.2% of its GDP (UNISDR, 2015). This preliminary work focuses on the Chilean national electrical transmission system, called SEN (*Sistema Eléctrico Nacional*), which serves 98.5% of the Chilean population. It describes the development of a Chilean EPN model and presents an analysis framework to assess its resilience defined as "the ability of the system to sustain or restore its basic functionality following a risk source or an event" (SRA, 2015).

Resilience analyses of EPNs have been the subject of numerous studies in the last decade (e.g., Fang et al., 2015, Mensah and Dueñas-Osorio, 2016; Nan and Sansavini, 2017; Panteli and Mancarella, 2017); however, few works have focused on the resilience of EPNs under earthquakes. In this context, some authors have looked for retrofit strategies to increase EPN's resilience against earthquakes (Romero et al., 2015) or modeled the restoration process by means of discrete-event simulation models (Cağnan et al., 2006); other authors have estimated seismic risk and resilience of EPNs by resorting to Monte Carlo simulations (e.g., Shinozuka et al., 2007; Poulos et al., 2017). In a probabilistic framework, seismic resilience is determined by analyzing the underserved demand caused by an earthquake until full restoration of the EPN, whereas seismic risk is usually expressed in terms of expected annual losses and mean annual frequencies of exceedance of decision variables considering all possible earthquakes (Poulos et al., 2017).

A critical input required to perform resilience analysis of EPNs is a model of the EPN with identifiable bounds, topology, components, and relevant electrical data. Herein, considerable effort was spent toward building the Chilean EPN model using several official Chilean data sources. To the best of our knowledge, it is the first SEN's

Proceedings of the 29th European Safety and Reliability Conference.
Edited by Michael Beer and Enrico Zio

Published by Research Publishing, Singapore.
ISBN: 978-981-11-2724-3; doi:10.3850/978-981-11-2724-3_0558-cd

model at a high resolution level for resilience analysis purposes.

The resilience of the EPN to a seismic event is assessed in four main steps (Poulos et al., 2017): (1) generation of local intensity levels at the component geographical locations, characterized here by peak ground acceleration (PGA); (2) evaluation of the earthquake impact on the EPN components using fragility functions; (3) evaluation of component recovery time using downtime distributions; and (4) evaluation of the EPN's performance by means of a Direct Current-Optimal Power Flow (DC-OPF) model until service is fully restored. Resilience is then expressed in terms of Unsupplied Energy (UE) and the time needed to recover full performance in the system. This paper illustrates the use of the model by assessing the resilience for a single earthquake event with a particular plausible scenario of component structural damage and recovery times. Future work will focus on computing seismic risk and resilience using multiple seismic scenarios with efficient Monte Carlo simulation techniques. Indeed, this is a first step of a larger project devoted to foresee, prevent, mitigate and better recover the Chilean EPN functionality losses during earthquakes.

The remainder of the paper is organized as follows. Section 2 introduces the Chilean EPN and describes the process of data collection. The representation and modeling of the Chilean EPN is presented in Section 3, and Section 4 describes the methodology for resilience evaluation under a single earthquake scenario. Section 5 presents preliminary results and discusses critical aspects of the analysis framework adopted. Finally, Section 6 provides conclusions and ideas for future work.

2. Chilean Electric Power Network Description and Data Collection

Three main EPN systems currently operate in Chile: the national electrical system (SEN), and the Aysén and Magallanes electrical systems in the southern part of the country. This work focuses on the SEN, which covers most of the national territory from the city of Arica in the north to the Chiloé Island in the south and serves 98.5% of the Chilean population (Coordinador, 2019a).

This work represents and models the SEN by means of a network-based approach that accounts for the operation of the system (see Section 3), which requires gathering both topological and electrical data. Topological data are needed to identify the components and their physical/functional interconnections, whereas electrical data are needed to simulate the system's operation. For the sake of simplicity, this work considers hourly historical load (hourly load profile) and power generation from renewable sources (hourly generation profile) for a year, which avoids the use of complicated load and weather forecasting models. Year 2017 was taken as a reference since it was the most recent year available with data when this study started.

The data was retrieved from official Chilean databases; specifically, from the National Electrical Coordinator (Coordinador, hereafter), which has been considered as the reference source herein (Coordinador, 2019b), the Ministry of Energy (2019), and the National Energy Commission through its Energía Abierta platform (Energía Abierta, 2019), which were used to complement or correct data.

It is relevant to mention that though SEN has experienced structural modifications in 2017, such as the installation of new substations, transmission lines, and power plants, the system topology will be assumed the same during the entire year.

The main difficulties encountered in the data collection process are attributed to: 1) incomplete databases, e.g., lack of system components, geographical or technical data related to the components, and hourly historical generation/load profiles; 2) inconsistent databases with different system component names in different databases and repeated component names within the same database; 3) errors in geographical location, load and transmission line data; and 4) data preprocessing to estimate, e.g., maximum generation capacities of power plants in disaggregated form for each unit inside them.

Sections 2.1 through 2.4 describe the data collected for the EPN components, and Figure 1 (parts a. and b.) presents the power plants, substations, and transmission lines in Chile.

2.1 *Power plants*

Power plants are composed by different units that can operate with various fuels. For this reason, power plant data were collected at the unit level. The data considered for power plants are: installed maximum generation capacity, starting operation date, substation of connection, hourly generation profile during 2017, and generation cost. Technical information related to units, such as the maximum generation capacity, was taken from the Coordinador (2019b), whereas historical generation profiles were retrieved from Energía Abierta (2019). In case of inconsistencies between the databases, say units reported only in one database, the database of Energía Abierta was considered since it provides the historical generation profile.

The collected data shows that 500 generation units were in operation during 2017 with a total installed capacity of 21900 MW, consisting in a wide variety of primary energy sources, coal

(18.6%), oil (15.6%), natural gas (18.5%), biomass (1.9%), water (30.6%), wind (5.1%), solar (9.5%), and geothermical energy (0.2%).
The generation cost of a unit g at a given time, c_g^{gen}, is computed by considering the variable generation cost associated with the fuel, $c_g^{var\_f}$, and with other materials and processes, $c_g^{var\_nf}$, such as water, oil, filters, spare parts, and maintenance checks (CNE, 2018):

$$c_g^{gen} = \left(c_g^{var\_f} + c_g^{var\_nf}\right) \cdot E_g \quad (1)$$

where E_g is the energy generated by unit g. Variable fuel costs of each unit were computed as the product of the fuel cost and the specific fuel consumption of the unit, whereas variable costs not related to the fuel, $c_g^{var\_nf}$, were retrieved from CNE (2018). Fixed generation costs were not considered since unit commitment was not performed.

2.2 *Substations*

Substations are a key element in electric power systems since they form essential links between power plants, transmission lines and loads; they can have several functions, such as to step-up and -down voltage levels to allow the connection between transmission lines of different voltages. Within the substation set, tap-offs –small substations that allow a simple connection from an electric line for energy withdrawal or power supply– were included.
Four databases given by the Coordinador (2019b) were considered to identify and localize the Chilean substations: 1) a substation database that provides geographical coordinates, starting operation dates, and other technical information of most Chilean substations; 2) a load database that gives the hourly load profile of substations (Coordinador, 2018); 3) a transmission line database that identifies the connections among substations including also some substations and tap-offs not considered in the first database; and 4) a power plant database that reports the information about their connecting substations, i.e., the substations used by power plants to inject power into the grid, which are not always present in the substation and transmission line databases. Each of these databases was incomplete in some aspects, and hence they were consolidated into a single consistent database. In general, priority for the substation identification was given to the load, transmission line, and power plant databases, neglecting substations in the first database that do not have load or are not connected to the network or a power plant. In addition, the database of the Ministry of Energy (2019) was used to retrieve missing geographical coordinates. However, assumptions related to the location of substations not given neither in the first database nor in the database of the Ministry of Energy had to be done, say unknown locations of connecting substations were set equal to locations of their associated power plants, and minor substations such as tap-offs in the middle of a line were in some cases neglected. In this process of substation identification, spatial attention was paid to the Valparaiso and Metropolitan regions of Chile, which are the focus of this study. At the end of the process, 994 substations were identified.

2.3 *Transmission lines*

Transmission lines connect all substations and efficiently transport electricity generated by power plants to loads. The transmission line database, where lines are identified by the substation names at their ends, was taken as reference to identify network connections and obtain the technical characteristics of the lines, such as length, capacity, and reactance (Coordinador, 2019b). However, this database is incomplete and new lines had to be added manually to connect all the substations identified in Section 2.2. This process was laborious and carried out using the electrical unilinear diagram and a map of locations provided by the *Coordinador* (2019b). When information about the connection of a substation to the network could not be found, it was assumed that this isolated substation was connected to the closest substation in the network with a line characterized by infinite capacity, values of reactance and voltage consistent with those of the adjacent line, and a length given by the Euclidean distance between the two substations. Moreover, when a small substation between connections of two or three substations was not considered (see Section 2.2), equivalent lines were defined with capacity and reactance equal to the minimum capacity and equal to the sum of the reactance of the lines connected in series, respectively. Finally, it is worth mentioning that the capacity of 48 transmission lines have been increased to a very high number during the process of the network validation to avoid the occurrence of load shedding in normal operation. Future work will be devoted to perform a deeper network validation to identify possible errors in the line capacity data.
This data processing resulted in that the 994 substations identified in Section 2.2 were connected by 1195 transmission lines, with voltage levels varying from 11 to 500 kV. Few transmission lines (41) have low voltage which is equal or lower than 23 kV.

2.4 *Loads*

Loads represent the electric power demand of residential, commercial, and industrial customers. In the load database provided by the Coordinador (2018), the distinction between two types of

clients (i.e., regulated and free clients) was made on the basis of different pricing conditions given by the Chilean law (CNE, 2019). In principle, regulated clients represent residential and commercial customers, while free clients are industrial customers. In the database, load was given for each bus at different voltage levels and for each client. The data was then aggregated to obtain the total load at a substation level for regulated and free clients. The lack of load data associated with some buses was complemented with the database provided by the Coordinador (2019c).

After processing the load data, the total 2017 load was found to be 68,526 GWh, with 48% required by regulated clients and the remaining 52% by free clients. The peak load reached in 2017 was 10.0 GW.

Fig. 1. Map of the Chilean EPN: a) power plants; and b) substations and transmission lines. Notice that the substation outside Chile is in Argentina.

3. Chilean Electric Power Network Representation and Modeling

3.1 *System representation*

The Chilean electric power system is represented by a network-based approach with two levels of system representation. In the first level, nodes represent different EPN components, i.e., substations and power plants, with their real geographical coordinates; and links represent the connections between these components. This representation, given by the integration of Figure 1a. and 1b., is used to assess the level of earthquake damage of system components. A second level representation is adopted to run a power flow model (see Section 3.2) and determine system functionality. In this more abstract representation, nodes represent substations that may include power generation and/or load, and links are the transmission lines connecting substations.

3.2 *System modeling*

The performance of the Chilean EPN in terms of unsupplied energy was evaluated by solving the power in normal steady state operation through the Direct Current – Optimal Power Flow (DC-OPF) model, which is typically adopted in practice for transmission networks (Gan et al., 2013).

A fundamental step in assessing the system performance after an earthquake is to include the component damage states in the DC-OPF model. Therefore, the states of structural damage and functionality of the system components need to be determined first in order to assess the system's operation and network performance. Section 3.2.1 provides the relation between structural damage and functionality at component level, and Section 3.2.2 presents the DC-OPF optimization model used to evaluate the performance at a system level.

3.2.1 *Structural damage and functionality at component level*

As a first approach, it was assumed that only substations and power plants can be directly damaged by the occurrence of an earthquake, whereas damage in lines, being aerial elements, can be neglected and their failure is only a consequence of the substation's failure. The structural state of power plants, u_g^{str}, and substations, u_s^{str}, can assume five levels of damage, from no damage to complete damage, as illustrated in Section 4.2. However, given that the relation between structural damage and functionality is difficult to establish, the operation of a component was assumed to stop if it has any

level of structural damage. The functionality of power plants and substations is then represented by binary variables, u_g^{op} and u_s^{op}, respectively, which are 0 if the facilities are not working due to a structural damage and 1 if they are in operation. A further assumption for a damaged substation is that all lines connected to it are disconnected from the network, $u_l^{op} = 0$. Thus, a transmission line is considered in operation, $u_l^{op} = 1$, only if it connects two substations in operation.

3.2.2 *DC-OPF model*

The DC-OPF model consists of a linear relation between power flow through lines and power injection at generator nodes. The problem formulation is given by Eqs. (2)-(9) for a specific hour of interest.

$$\min\left\{\sum_{g \in \mathcal{G}} P_g \cdot c_g^{gen} + \sum_{n \in \mathcal{N}} LS_n \cdot c_n^{LS}\right\} \quad (2)$$

$$\sum_{g \in \mathcal{G}(n)} P_g + LS_n - \tau^{loss} D_n + \sum_{l \in \mathcal{L}(n)} f_{l,n}^{in} - \sum_{l \in \mathcal{L}(n)} f_{l,n}^{out} = 0\,, \quad \forall\, n \in \mathcal{N} \quad (3)$$

$$0 \le P_g \le P_g^{max} \cdot u_g^{op}\,, \quad \forall\, g \in \mathcal{G}^T, \mathcal{G}^T \subset \mathcal{G} \quad (4)$$

$$0 \le P_g \le P_g^{hist} \cdot u_g^{op}\,, \quad \forall\, g \in \mathcal{G}^R, \mathcal{G}^R \subset \mathcal{G} \quad (5)$$

$$0 \le LS_n \le D_n\,, \quad \forall\, n \in \mathcal{N} \quad (6)$$

$$f_l = \frac{S_0}{x_l} \cdot (\theta_n - \theta_h) \cdot u_l^{op}\,, \quad \forall\, l \in \mathcal{L}, n, h \in \mathcal{N}(l) \quad (7)$$

$$-f_l^{max} \le f_l \le f_l^{max}\,, \quad \forall\, l \in \mathcal{L} \quad (8)$$

$$\theta_{n_{ref}^{isl}} = 0\,, \quad n_{ref}^{isl} \in \mathcal{N}, isl = 1, \dots, N_{isl} \quad (9)$$

The objective function given in Eq. (2) minimizes the generation cost and the load shedding; specifically, P_g is the power generated by unit g; $\mathcal{G}$ is the set of power plants; c_g^{gen} is the cost of power generation of the unit g, as given by Eq. (1); LS_n is the load shedding of the substation n; $\mathcal{N}$ is the set of substations; and c_n^{LS} is the service interruption cost of substation n due to load shedding. The service interruption costs, c_n^{LS}, are assumed to be a very large value, i.e., 1000 US$/MWh, to penalize the occurrence of load shedding in the optimization problem.

Eqs. (3)-(9) represent the constraints of the OPF problem. Eq. (3) represents the power balance at each node n, where $\mathcal{G}(n)$ is the set of power plants connected to node n, D_n is the demand of the node n, τ^{loss} is the power loss represented through the load that are assumed to be constant, $f_{l,n}^{in}$ and $f_{l,n}^{out}$ represent the flow through line l that enters and leaves node n; and $\mathcal{L}(n)$ is the set of lines connecting node n. Eqs. (4)-(5) represent power plant capacity constraints for thermal (Eq. (4)) and renewable energy power plants (Eq. (5)), P_g^{max} is the maximum power that can be generated by the unit g, $\mathcal{G}^T$ is the set of thermal power plants, P_g^{hist} is the historical power generated by the unit g, and $\mathcal{G}^R$ is the set of renewable energy power plants. Eq. (6) represents the constraints associated to load shedding in each node, which cannot be higher than the demand of the node D_n. Eq. (7) represents the flow through line l, where θ_n and θ_h, are the voltage angles at the end nodes of line l with $n, h \in \mathcal{N}(l)$; $\mathcal{N}(l)$ is the set of end nodes of line l; $\mathcal{L}$ is the set of all lines; S_0 is the base power, set to 100 MVA in this work; and x_l is the reactance of the line l. Eq. (8) represents a line capacity constraint, where f_l^{max} is the maximum capacity of line l. Finally, Eq. (9) sets the voltage angle of the reference node(s) to zero: when the network is fully connected, $isl = 1$, one reference node is identified, otherwise when N_{isl} islands are generated, N_{isl} reference nodes should be identified and their voltage angles set to zero.

4. Seismic Resilience Assessment

In order to evaluate resilience of the EPN system exposed to a single earthquake scenario, the earthquake event of interest is identified first; then, its impact on all the system components is assessed, and their recovery time estimated; and, finally, the measure of resilience is calculated. Each of these steps is described next in more detail.

4.1 *Earthquake scenario*

The system was subjected to a Mw 8.5 earthquake scenario with the same epicenter as the Mw 8.0 1985 Algarrobo earthquake in central Chile. PGA values at all sites, **IM**, were sampled using the ground motion prediction model (GMPM) developed by Abrahamson et al. (2016):

$$\ln \boldsymbol{IM} = \ln \overline{\boldsymbol{IM}} + \boldsymbol{\sigma} \circ \boldsymbol{\varepsilon} + \tau\eta \quad (10)$$

where $\overline{\boldsymbol{IM}}$ is the vector of median PGAs at all sites given by the GMPM, which depends on earthquake magnitude, the distances from each site to the rupture plane, and local soil conditions characterized by the average shear wave velocity in the top 30 m of soil (Vs30); $\boldsymbol{\sigma}$ is the vector of intra-event standard deviation term for all sites, given by the GMPM; τ is the inter-event standard deviation term from the GMPM; $\circ$ denotes the entrywise product of vectors; η is the inter-event normalized residual, which has a standard normal distribution but was arbitrarily chosen as zero for the example earthquake; and $\boldsymbol{\varepsilon}$ is the vector of intra-event normalized residuals for all sites. The work of Jayaram & Baker (2008) shows that intra-event residuals follow a multivariate normal distribution with zero mean and unitary standard deviation: $\boldsymbol{\varepsilon} \sim N(\mathbf{0}, \boldsymbol{\Sigma})$.

Since intra-event residuals are also spatially correlated, several correlation structures have been proposed that depend on the distances between sites. The covariance matrix of the multivariate normal distribution, $\boldsymbol{\Sigma}$, was constructed using the model calibrated by Goda & Atkinson (2010) with Japanese records:

$$\Sigma_{ij} = \max\left[0;\, \gamma \exp\left(-\alpha {d_{ij}}^{\beta}\right) - \gamma + 1\right] \quad (11)$$

where α, β and γ are calibration parameters that depend on structural period; and d_{ij} is the distance between sites.

4.2 *Seismic fragility and restoration functions*

Once PGA values are computed for each network component, the earthquake impact on the components can be estimated by means of fragility curves (Cavalieri et al., 2014; Poulos et al., 2017). A seismic fragility curve is defined as the conditional probability of failure for any given ground motion level (EPRI, 2013), where "failure" means generically "degree of damage" when considering different levels of damage of the components (PEER, 2011). This work adopts the fragility curves provided by FEMA (2003) for anchored facilities with low (between 34.5 kV and 150 kV), medium (between 150 kV and 350 kV), and high (above 350 kV) voltage substations, and for small (<200 MW) and medium/large (>200 MW) thermal power plants. For each facility, four fragility curves are identified representing five states of structural damage, i.e., no damage, slight/minor, moderate, extensive, and complete damage (FEMA, 2003).

The recovery time of damaged components are estimated by means of normal probability distributions (FEMA, 2003). Each damage state has different restoration distributions. Thus, a facility with slight damage will recover faster than one with complete damage.

4.3 *Monte Carlo simulation*

The main steps to evaluate the resilience of EPNs under the occurrence of an earthquake by using Monte Carlo simulation are the following:

i. Selection of a seismic scenario and estimation of ground motion intensities at all sites where EPN components are located using a GMPM (Section 4.1)
ii. Estimation of component damage using seismic fragility curves (Section 4.2)
iii. Estimation of component recovery time using downtime functions (Section 4.2)
iv. Evaluation of the EPN performance (Section 3.2) at the time of earthquake occurrence and simulation of the hourly operation until the system performance is fully recovered.

This procedure will be used in future work to compute seismic risk by repeating steps i.-iv. for a large number of different earthquake scenarios.

5. Preliminary Results and Discussion

Figure 2 a. shows a PGA field from a single PGA sample of the earthquake scenario, achieved by sampling $\boldsymbol{\varepsilon}$ once (see Section 4.1). The Figure only shows central Chile since the components outside this region were subjected to negligible accelerations. The scatter in the PGA values is explained mainly by the sampling of different intra-event residuals at each location, but also by the differences in local Vs30 values, which were obtained from a USGS database (Allen and Wald, 2007). Figure 2 b. presents a possible scenario of structural damage states of EPN components, sampled using the PGA field of Figure 2a. Figure 2 c. shows a possible scenario of the recovery times of damaged components.

The damage state and the recovery time of components shown in Figures 2b. and 2c. were used to simulate the operation of the EPN following the earthquake using the DC-OPF model of Section 3.2.2, resulting in a total amount of unsupplied energy of 307.6 GWh and a system recovery time of 1125 hours, i.e., approx. 47 days. Figure 2d. illustrates the restoration of service over time in terms of percentage of energy demand being satisfied from the occurrence of the earthquake until the full system recovery. Notice that the curve is not monotonically increasing due to the hourly variability of the total demand of the system.

The analysis framework for resilience of EPNs exposed to the occurrence of earthquake scenarios, illustrated in this work, presents some critical aspects that need to be discussed. First, accurate fragility curves for the EPN components under analysis are essential to achieve realistic results. In this work, fragility curves are taken from the scientific literature (FEMA, 2003), as typically done in this kind of studies (Poljansek et al., 2012; Poulos et al., 2017). However, the fragility curves adopted are related to substations and power plants in the United States, which may present different characteristics from the EPN components in Chile and are subjected to different types of earthquakes. The same issue applies to the restoration functions, which were also taken from FEMA (2003).

Moreover, the relation between structural damage and component functionality is another critical part of this work. Indeed, it is very difficult to associate a level of structural damage with a level of functionality at a component level. In FEMA (2003), for example, the moderate damage state for substations is defined as "the failure of 40% of disconnect switches, or the failure of 40% of circuit breakers, or the failure of 40% of transformers, or by the building being in moderate damage state", but how can this definition of structural damage be translated into substation functionality? For the sake of simplicity, this work assumed a binary functionality state where any structural damage level leads to full interruption of the substation's operation; then, the multistate structural damage is only used to estimate the recovery time of the component: higher damage states result in longer recovery times.

Furthermore, it was assumed that transmission lines cannot be directly damaged by the earthquake, with their failure and recovery depending only on the failure and recovery of the

substations connected by them. The issue of defining a proper structural model for system components and identifying the corresponding functionality should be carefully addressed in future work. However, it is worth mentioning that the adopted analysis framework allows including this modeling improvement through the functional state variables (u_g^{op} and u_l^{op}) used in the DC-OPF model. It is interesting to notice that these state variables couple the structural and electrical engineering disciplines.

Finally, the time required to solve the DC-OPF problem for a single hour is relatively low, in average 0.2 seconds by using Gurobi optimizer on Python on an Intel Xeon E5-2660 v4 2.0 GHz processor. However, assessing the seismic risk of the system would require a high number of earthquake scenarios, and the DC-OPF problem needs to be solved for each hour until the full recovery of the system is achieved. For illustration purposes, if 10,000 seismic scenarios were used with an average recovery time of 60 days, the complete assessment would require 33 days to complete. Thus, the computational time is an issue that needs to be addressed in future work.

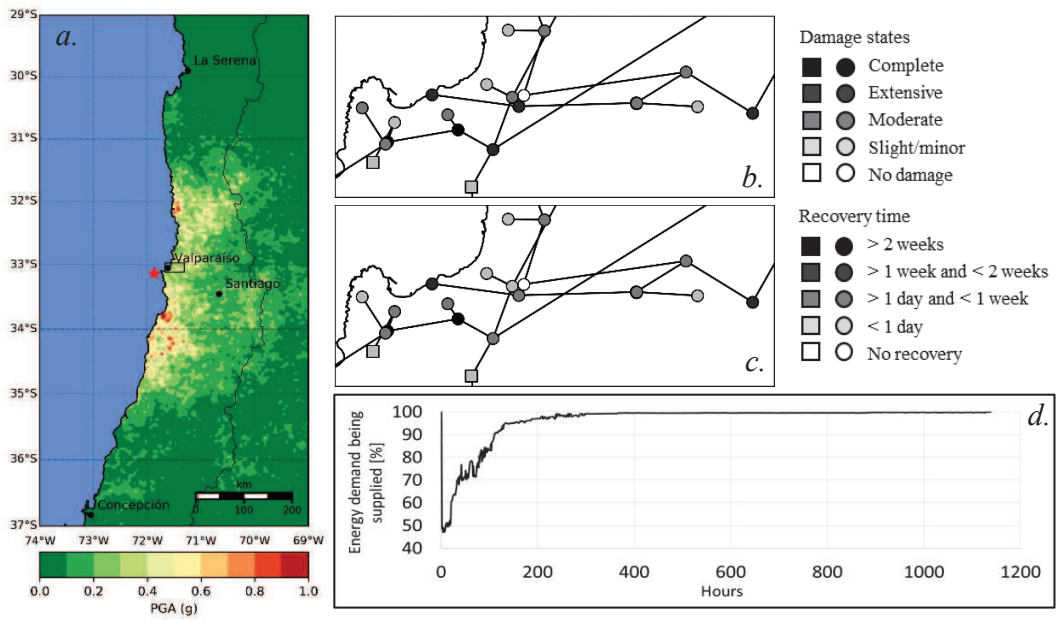

Fig. 2. Results of a single simulation from the selected Mw 8.5 earthquake scenario: a) PGA map in units of g (the red star denotes the earthquake epicentre, the rectangular represents the zoom considered in Fig. 2 b.-c.); b) structural damage states of EPN components; c) recovery time of the damaged components; and d) restoration of service over time in terms of percentage of energy demand being supplied. In Figures b.-c., squares and circles represent power plants and substations, respectively; links represent transmission lines.

6. Conclusion

This work focused on the Chilean EPN earthquake resilience. An in depth topological and electrical data collection process was first carried out to characterize and model the EPN under a framework of resilience assessment. The model was then used to evaluate a single seismic scenario of interest by sampling earthquake intensities, structural damage, and recovery times at a component level, and then simulating the EPN operation to calculate the corresponding unsupplied energy until full system recovery is achieved. The original contributions of this work are related to the construction of a consistent Chilean EPN model at a high level of resolution for resilience analyses under the occurrence of severe earthquakes, and also to the discussion of some critical aspects of the framework for future research developments. Future work will be devoted to carry out a Monte Carlo-based seismic risk assessment of the Chilean EPN using multiple earthquake scenarios consistent with the seismic hazard of the country. Results from these analyses would help refine future investment decisions and improve seismic resilience of EPNs.

Acknowledgement

This study has been sponsored by the Chilean National Commission for Scientific and Technological Research (CONICYT) under Fondecyt grant #3180464, # 1170836, and #11170423, and by the Chilean National

Research Center for Integrated Natural Disaster Management CONICYT/FONDAP/15110017 (CIGIDEN). The authors also wish to thank Mr. Sebastián Castro for providing constructive support in the process of data collection.

References

Allen, T.I. and D.J. Wald (2017). Topographic Slope as a Proxy for Seismic Site-Conditions (VS30) and Amplification Around the Globe. U.S. Geological Survey Open-File Report 2007-1357, Reston, Virginia.

Araneda, J.C., H. Rudnick, S. Mocarquer, P., and Miquel (2010). Lessons from the 2010 Chilean earthquake and its impact on electricity supply. *International Conference on Power System Technology*.

Çağnan, Z., R. A. Davidson, and S. D. Guikema (2006). Post-earthquake restoration planning for Los Angeles electric power. *Earthquake Spectra 22(3)*, 589–608.

Cavalieri, F., P. Franchin, J.A.M. Buriticá Cortés, and S. Tesfamariam (2014). Models for seismic vulnerability analysis of power networks: comparative assessment. *Computer-Aided Civil and Infrastructure Engineering 29*, 590-607.

CNE (2018). Informe de costos de tecnologías de generación. Informe anual. Comisión Nacional de Energía.

CNE (2019). www.cne.cl/tarificacion/electrica/ Comisión Nacional de Energía. Last access March 2019.

Coordinador (2018). Database provided by email by the Coordinador Eléctrico Nacional in May 2018.

Coordinador (2019a). www.coordinador.cl/sistema-electrico/ Coordinador Eléctrico Nacional. Last access March 2019.

Coordinador (2019b). https://infotecnica.coordinador.cl/ Coordinador Eléctrico Nacional. Last Access March 2019.

Coordinador (2019c). https://aplicaciones-sic.coordinador.cl/redcdec/ Coordinador Eléctrico Nacional. Last Access March 2019.

Dueñas-Osorio, L. and A. Kwasinski (2012). Quantification of Lifeline System Interdependencies after the 27 February 2010 Mw 8.8 Offshore Maule, Chile, Earthquake. *Earthquake Spectra 28*, S581-S603.

Energía Abierta (2019). http://energiaabierta.cl/ Energía Abierta. Last access March 2019.

EPRI (2013). Seismic probabilistic risk assessment - Implementation guide. Final Report 3002000709, EPRI, Palo Alto, CA.

Fang, Y., N. Pedroni, and E. Zio (2015). Optimization of Cascade-Resilient Electrical Infrastructures and its Validation by Power Flow Modeling. *Risk Analysis 35(4)*, 594–607.

FEMA (2003). Hazus-MH 2.1 Technical Manual. Department of Homeland Security, Federal Emergency Management Agency, Mitigation Division Washington, D.C.

Goda, K., and G.M. Atkinson (2010). Intraevent spatial correlation of ground-motion parameters using SK-net data. *Bulletin of the Seismological Society of America 100(6)*, 3055-3067.

Jayaram, N. and J.W. Baker (2008). Statistical tests of the joint distribution of spectral acceleration values. *Bulletin of the Seismological Society of America 98(5)*, 2231-2243.

Kröger, W. and E. Zio (2011). *Vulnerable systems*. Springer-Verlag London.

Mensah, A. F. and L. Dueñas-Osorio (2016). Efficient Resilience Assessment Framework for Electric Power Systems Affected by Hurricane Events. *Journal of Structural Engineering 142(8)*.

Ministry of Energy (2019) sig.minenergia.cl/sig-minen/moduloCartografico/composer/ Ministerio de Energía. Last Access March 2019

Nan, C. and G. Sansavini (2017). A quantitative method for assessing resilience of interdependent infrastructures. *Reliability Engineering and System Safety 157*, 35–53.

NRC (2013). The Resilience of the Electric Power Delivery System in Response to Terrorism and Natural Disasters: Summary of a Workshop. National Research Council. Washington, DC: The National Academies Press.

Panteli, M. and P. Mancarella (2017). Modeling and Evaluating the Resilience of Critical Electrical Power Infrastructure to Extreme Weather Events. *IEEE Systems Journal 11(3)*, 1733-1742.

PEER (2011). A Bayesian Network Methodology for Infrastructure Seismic Risk Assessment and Decision Support. PEER Report 2011/02. Pacific Earthquake Engineering Research Center College of Engineering, University of California, Berkeley.

Poljansek K., F. Bono, and E. Gutiérrez (2012). Seismic risk assessment of interdependent critical infrastructure systems: the case of European gas and electricity networks. *Earthquake Engineering and Structural Dynamics 41*, 61–79.

Poulos, A., S. Espinoza, J.C. de la Llera, and H. Rudnick (2017). Seismic Risk Assessment of Spatially Distributed Electric Power Systems. *16th World Conference on Earthquake Engineering*, Santiago, Chile.

Romero, N., L.K. Nozick, I. Dobson, N. Xu, and D. A. Jones (2015). Seismic retrofit for electric power systems. *Earthquake Spectra 31(2)*, 1157–1176.

Shinozuka, M., X. Dong, T.C. Chen, and X. Jin (2007). Seismic performance of electric transmission network under component failures. *Earthquake Engineering and Structural Dynamics* 36, 227–244.

Southwell, P. (2014). Disaster Recovery within a Cigre Strategic Framework: Network Resilience, Trends and Areas of Future Work. Cigre.

SRA (2015). SRA glossary. Society for Risk Analysis. Committee on Foundations of Risk Analysis.

UNISDR (2015). Global Assessment Report on Disaster Risk Reduction. Country risk profile. United Nations Office for Disaster Risk Reduction.